# INITIAL RESULTS: AN ULTRA-LOW-BACKGROUND GERMANIUM CRYSTAL ARRAY

Martin E. Keillor, Craig E. Aalseth, Anthony R. Day, Luke E. Erikson, James E. Fast, Brian D. Glasgow, Eric W. Hoppe, Todd W. Hossbach, Brian J. Hyronimus, Harry S. Miley, Allan W. Myers, and Allen Seifert

Pacific Northwest National Laboratory

Sponsored by the National Nuclear Security Administration

Award No. DE-AC05-RLO1830/PL10-CASCADES-NDD05

## ABSTRACT

Treaty verification techniques, environmental surveillance, and physics experiments continue to require increased sensitivity for detecting and quantifying radionuclides of interest. This can be accomplished with new detector designs that establish high detection efficiency and reduced instrument backgrounds. Current research is producing an intrinsic germanium (HPGe) array designed for high detection efficiency, ultra-low-background performance, and sensitive γ-γ coincidence detection. The system design is optimized to accommodate filter paper samples, e.g., samples collected by the Radionuclide Aerosol Sampler/Analyzer (RASA). The system will provide high sensitivity for weak collections on atmospheric filter samples (e.g., $< 10^5$ fissions), as well as offering the potential to gather additional information from higher-activity filters using gamma cascade coincidence detection. The first of two HPGe crystal arrays in ultra-low-background vacuum cryostats has been assembled, with the second in progress. Traditional methods for constructing ultra-low-background detectors were followed, including use of materials known to be low in radioactive contaminants, use of ultra-pure reagents, and use of a clean room assembly. The cryostat is constructed mainly from copper electroformed into near-final geometry at Pacific Northwest National Laboratory. Details of the detector assembly, vacuum and thermal performance testing, and initial measurement results are presented.

| 1. REPORT DATE | 2. REPORT TYPE | 3. DATES COVERED |
| --- | --- | --- |
| **SEP 2010** | | **00-00-2010 to 00-00-2010** |

| | |
| --- | --- |
| 4. TITLE AND SUBTITLE<br>**Initial Results: An Ultra-Low-Background Germanium Crystal Array** | 5a. CONTRACT NUMBER<br>5b. GRANT NUMBER<br>5c. PROGRAM ELEMENT NUMBER |
| 6. AUTHOR(S) | 5d. PROJECT NUMBER<br>5e. TASK NUMBER<br>5f. WORK UNIT NUMBER |
| 7. PERFORMING ORGANIZATION NAME(S) AND ADDRESS(ES)<br>**Pacific Northwest National Laboratory,902 Battelle Boulevard,Richland,WA,99352** | 8. PERFORMING ORGANIZATION REPORT NUMBER |
| 9. SPONSORING/MONITORING AGENCY NAME(S) AND ADDRESS(ES) | 10. SPONSOR/MONITOR’S ACRONYM(S)<br>11. SPONSOR/MONITOR’S REPORT NUMBER(S) |

12. DISTRIBUTION/AVAILABILITY STATEMENT

**Approved for public release; distribution unlimited**

13. SUPPLEMENTARY NOTES

**Published in Proceedings of the 2010 Monitoring Research Review - Ground-Based Nuclear Explosion Monitoring Technologies, 21-23 September 2010, Orlando, FL. Volume II. Sponsored by the Air Force Research Laboratory (AFRL) and the National Nuclear Security Administration (NNSA). U.S. Government or Federal Rights License**

14. ABSTRACT

**Treaty verification techniques, environmental surveillance, and physics experiments continue to require increased sensitivity for detecting and quantifying radionuclides of interest. This can be accomplished with new detector designs that establish high detection efficiency and reduced instrument backgrounds. Current research is producing an intrinsic germanium (HPGe) array designed for high detection efficiency, ultra-low-background performance and sensitive γ-γ coincidence detection. The system design is optimized to accommodate filter paper samples e.g., samples collected by the Radionuclide Aerosol Sampler/Analyzer (RASA). The system will provide high sensitivity for weak collections on atmospheric filter samples (e.g., < 105 fissions), as well as offering the potential to gather additional information from higher-activity filters using gamma cascade coincidence detection. The first of two HPGe crystal arrays in ultra-low-background vacuum cryostats has been assembled, with the second in progress. Traditional methods for constructing ultra-low-background detectors were followed, including use of materials known to be low in radioactive contaminants, use of ultra-pure reagents, and use of a clean room assembly. The cryostat is constructed mainly from copper electroformed into near-final geometry at Pacific Northwest National Laboratory. Details of the detector assembly, vacuum and thermal performance testing, and initial measurement results are presented.**

15. SUBJECT TERMS

<table>
<tr><td colspan="3">16. SECURITY CLASSIFICATION OF:</td><td rowspan="2">17. LIMITATION OF ABSTRACT<br>Same as Report (SAR)</td><td rowspan="2">18. NUMBER OF PAGES<br>10</td><td rowspan="2">19a. NAME OF RESPONSIBLE PERSON</td></tr>
<tr><td>a. REPORT<br>unclassified</td><td>b. ABSTRACT<br>unclassified</td><td>c. THIS PAGE<br>unclassified</td></tr>
</table>

## OBJECTIVES

The objective for the "Radionuclide Laboratories " (RN Labs) project was to build an instrument utilizing two germanium arrays in ultra-low-background cryostats to surround the sample being measured. The follow-on "CASCADES" project aims to develop a multicoincidence data-analysis package and make robust fission-product demonstration measurements to establish system capabilities. The design and performance expectations for this instrument have been discussed previously (Keillor, et al., 2008, 2009). Each cryostat houses seven high-purity germanium crystals (HPGe); these cryostats are built using a limited set of materials known to have very low levels of radioactive impurities. The vast majority of each cryostat is made from pure copper (< 1μBq/kg, see Aalseth, et al., 2009) electroformed into near-final geometry at Pacific Northwest National Laboratory (PNNL) under class 1000 clean room conditions.

The instrument is designed to take advantage of low background performance, high detection efficiency, and γ-γ coincidence signatures to provide unprecedented gamma spectroscopy sensitivity. This effort is focused on improving gamma analysis capabilities for nuclear detonation detection (NDD) applications, e.g., nuclear treaty monitoring. The instrument also has the potential to contribute to basic nuclear physics research. For example, the potential for this detector to measure the half-life of predicted rare decay modes of $^{130}Te$ is being investigated.

## RESEARCH ACCOMPLISHED

This paper details assembly and initial characterization of the active anti-cosmic shield, assembly of the first seven-crystal array into its ultra-low-background cryostat, results of system thermal tests, and initial spectroscopic performance of the array. Initial spectral analysis results obtained with the analysis package in development under the CASCADES project are also presented.

### Active Anti-Cosmic Shield

To reduce backgrounds, an active cosmic veto shield composed of 12 BC-408 plastic scintillator panels was installed on the left, right, rear, and top surfaces of the passive lead shield. Panels will be added to the front and bottom sides to complete the active shield when the system is moved to the new shallow underground laboratory at PNNL; the move is scheduled for ~September 2010. The goal of this veto system is to detect and exclude cosmic-ray generated interactions within the germanium array. Each plastic panel is roughly 17.5" × 2" × 70" and makes use of a single photomultiplier tube to detect the scintillation light (widths and heights vary slightly to accommodate the shield dimensions). On each side protected by the active veto, the signals from three panels are combined into one Canberra model 2005 preampifier; the signal is subsequently read out by an XIA PIXIE-4 waveform digitizer. Figure 1 shows an example of a typical energy spectrum produced by a gain-matched side of the cosmic-ray veto (the red line is a fit to the cosmic-ray muon through-peak).

Various preliminary performance studies have been conducted with the current veto system. The time resolution of the system was of particular importance because the effects of a poor time resolution will increase the number of legitimate events improperly excluded during data collection. The waveform digitizer system also requires additional configuration to properly handle coincident signals across PIXIE-4 cards. In the system's initial configuration, our results suggest that the time resolution of the veto system is approximately 200 ns (see Figure 2) or better; planned changes to the signal processing should significantly improve this performance. The rejection efficiency for the active veto will be determined in the near future.

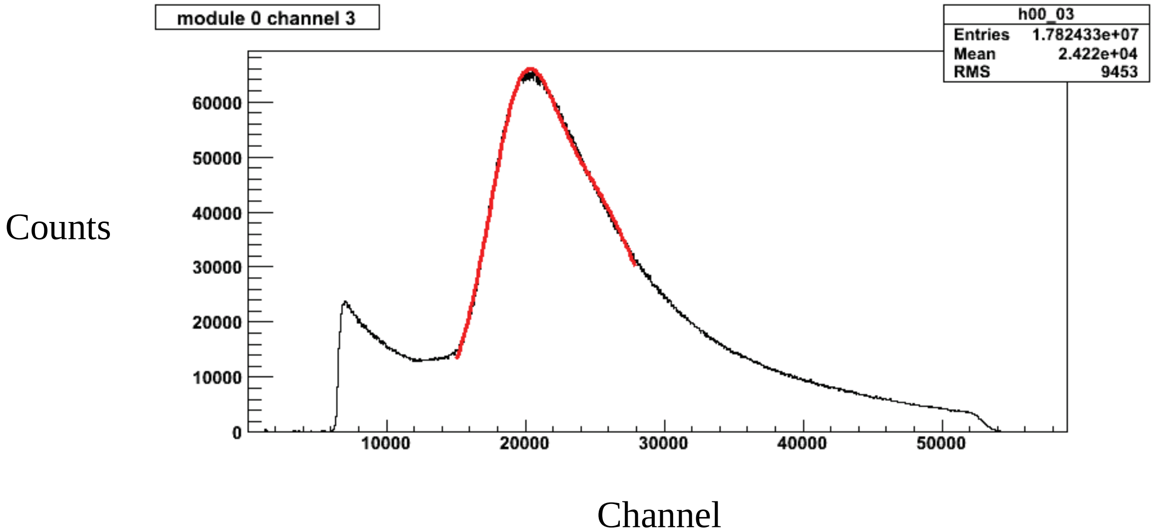


**Figure 1. Muon spectrum collected with three 2"-thick plastic scintillator panels "T'ed" together. These are the panels making up the active veto on the top surface of the lead shield. The lower energy threshold, as set in this figure, will accept some gamma background to ensure a high rate of muon exclusion.**

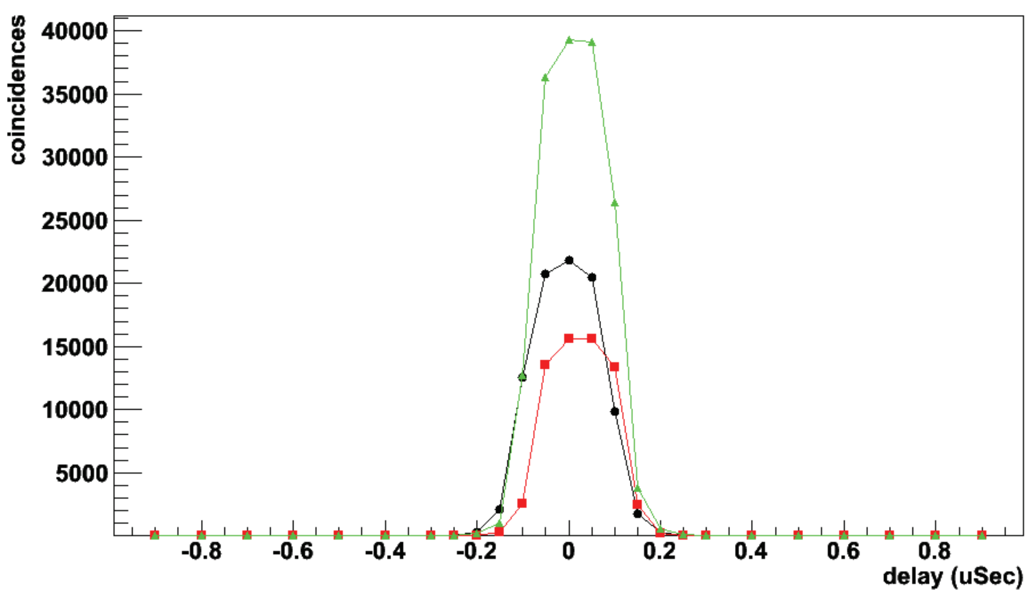


**Figure 2. Cosmic-ray coincidence data collected to investigate the single-card PIXIE time resolution for veto signals. Black circles are events collected in coincidence between panels on adjacent sides of the shield, red squares are between opposite sides of the shield, and the green triangles are coincident events from a side and the top of the shield.**

### Cryostat and HPGe Array Assembly

The first cryostat was initially assembled with all components except the IR shield and crystals in their mounting hardware. This includes installation of the low-background, front-end electronics package (LFEP); wiring; and preamplifiers. Cryostat vacuum and thermal performance were tested prior to installation of the seven HPGe crystals.

At MRR2009, we also reported challenges with electroforming of the thin IR shields and the domed entrance window for the system (Keillor, 2009). During the past year, both of these difficulties have been resolved. Our typical approach to removing an electroformed piece from its stainless steel mandrel is to heat the piece to ~ 300$^{o}$C, then rapidly cool it. We believe this heating process may contribute to accelerated electrochemical processes that result in the production of holes through thin pieces. This is specifically associated with parts electroformed on 304 stainless steel (SS) mandrels and has not been observed to affect parts on 316 SS mandrels. We have not completed a detailed study to verify this effect; however, we were able to solve the issues that delayed production of the IR shields. Rather than using the heating and quench process, electroformed IR shields were removed from their 304 SS mandrels by running a roller over the surface of the piece. This stretched the thin copper sufficiently to allow its release from the mandrel. The solution for the entrance window followed the method proposed in the MRR2009 paper: the thin window was electroformed separately, then e-beam welded into an annular plate to form the required part. This process allowed us to produce an entrance window that is ~0.04" (~ 1 mm) thick over a 5"-diameter window. Prior to installation of HPGe crystals, the cryostat was successfully cycled between vacuum and atmospheric pressure more than 15 times to verify that it would not fatigue and fail under vacuum or vacuum cycling. Figure 3 shows a cryostat assembled with the completed entrance window.

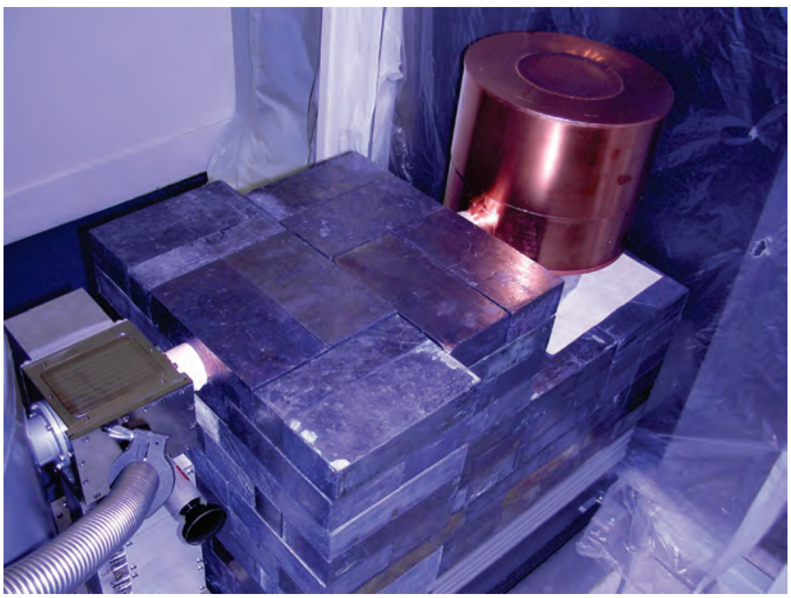

**Figure 3. Assembled cryostat with dished entrance window. The window is 5" in diameter and ~ 0.04" (1 mm) thick.**

Seven P-type coaxial HPGe crystals, nominally 63 mm in diameter by 70 mm high, were installed into the cryostat in mid-May 2010. This was completed in a clean room with the cryostat disconnected from the Dewar. The installation of each crystal assembly was relatively simple: signal wire was attached to the center connection of the crystal, then the HV wire was fed through the appropriate hole in the cold plate and attached. Following this, the crystal was placed on the cold plate and secured with electroformed copper nuts on the three posts. Once a crystal was secured, the cryostat was inverted to allow crimping of the signal wire to a lead attached to the gate of the LFEP. This sequence was repeated until all seven crystals were installed. Crystal installation was accomplished in a single session in the clean room, in less than 4 hours. Figure 4 shows a sequence of photos taken during the installation.

### Vacuum and Thermal Performance

For thermal testing, the cryostat was instrumented with four silicon resistance temperature detectors (RTDs) located along the cold path from the Dewar to the cold plate, as well as a Zener diode on the cold plate to allow injection of a known thermal load. Initial thermal tests showed that the cryostat did not cool sufficiently for operation of HPGe crystals. Two problems were corrected to improve cooling of the cold plate. First, a thermal short between the cold finger and cross arm was eliminated by modifying the copper piece that connects directly to the Dewar (the “nub”).

After elimination of the thermal short, the steel bolts holding a clamp that connects the nub to the cold finger were changed from 304 SS to 18-8 SS to eliminate loosening during thermal cycles. These changes allowed the cold plate to reach a temperature of 89.5K, deemed sufficient to proceed with installation of the HPGe crystals. We have noted that the aluminum-to-copper connection at the Dewar produces the largest single temperature change across a material interface ($\Delta T \sim 6$ K); at the next opportunity, we will attempt to improve thermal performance of this interface by inserting gold foil between the aluminum and copper.

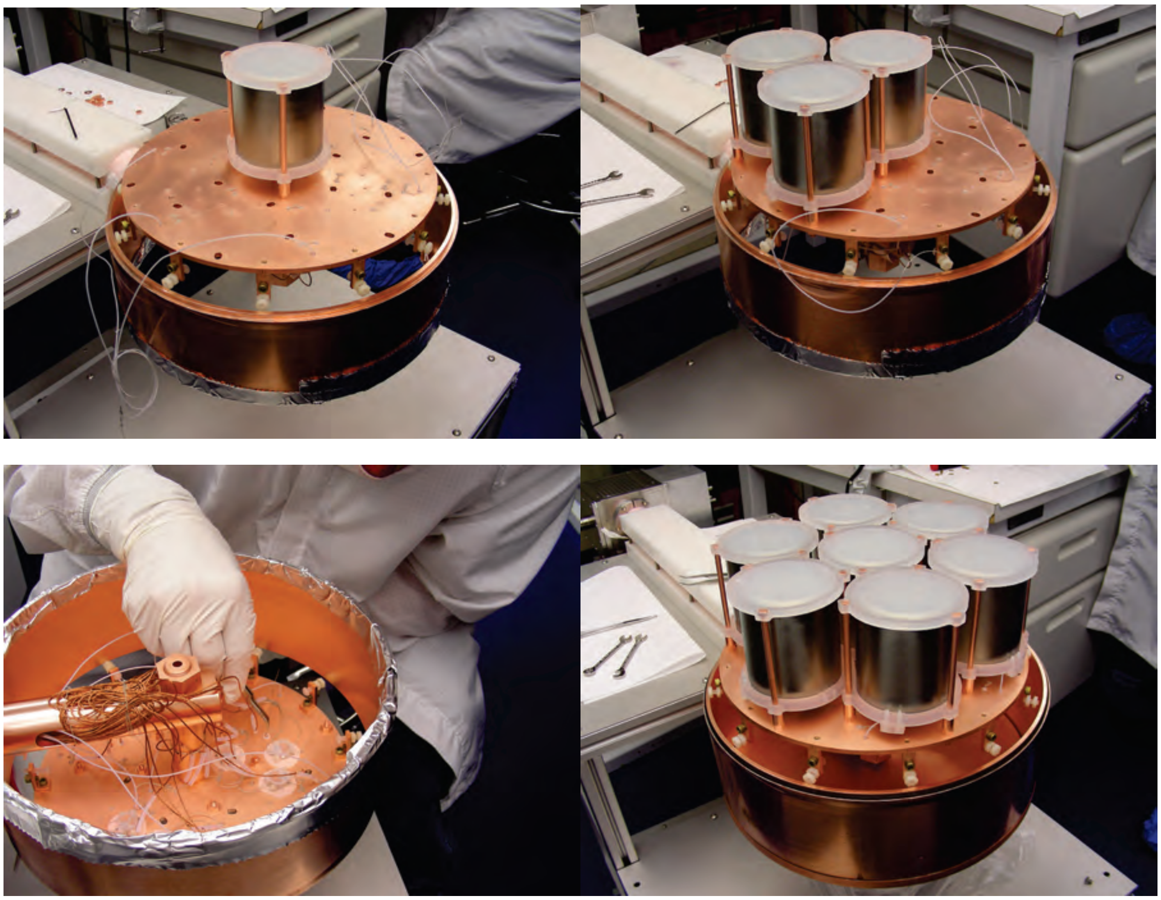

**Figure 4. This sequence of photos shows the progress of installation of the HPGe crystals. The frame in the lower left shows the cryostat inverted to allow easier access for crimping the signal wire.**

Cooling for the cryostat is provided by a liquid nitrogen (LN) Dewar, custom built by Technifab Corporation, with a 100-L capacity. Initial tests of this Dewar indicate that it uses about 1 kg of LN per day, with no external load. LN use with the cryostat attached is about 4 L/day, or 3.25 kg/day. Thus, the Dewar itself consumes about 2.3 W, while the cryostat represents a thermal load slightly above 5 W. This thermal load is consistent with our expectations. In the completed system, both cryostats will be cooled by the same Dewar; total LN use should be on the order of 7 L/day after installation of the second cryostat.

Results of previous vacuum testing were reported at MRR2009 (Keillor, 2009), and similar results were achieved with the fully assembled cryostat. Vacuum behavior was not as stable as expected during the first couple of attempts to cool the array after installation of the crystals; an epoxy patch was applied to a joint in the neck of the LN Dewar, but later discovery of a loose vacuum flange was the likely culprit. Despite the loose flange, the array was successfully cooled for testing and is currently holding in the temperature range of 82.5K–83.5K at the nub.

### Data Acquisition

The signal-processing path consists of PNNL LFEP sockets mounted near each crystal, on the opposite side of the cold plate, through Belden 8700 micro-coaxial cable (with insulation stripped to reduce background contribution) to a 50-pin vacuum feedthrough. Seven PGT RG-11 preamplifiers are mounted on a housing covering the outside of the vacuum feedthrough. Preamplifier power is supplied from Ortec 4003 preamplifier power supplies (NIM). Preamplifier signals are processed with a PXI crate holding five XIA PIXIE-4 digitizers. Software control of the data acquisition hardware uses an in-house PNNL data acquisition program called NYX (Cooper 2010). NYX provides much the same functionality as the Windows-based software supplied by XIA; however, it is based on Linux to provide a higher degree of stability. This acquisition system allows the user to specify different levels of data collection, with three key modes being (1) basic MCA-style spectra for each crystal, (2) time and energy list mode data, and (3) digitized waveform data for each observed pulse. The system also records coincident hit pattern information for modes 2 and 3.

### Development of Analysis Framework

When this system is complete, each measurement will contain data from 14 germanium crystals, coincidence hit pattern information, and the status of the active anti-cosmic shield. The availability of this robust dataset will make it possible to reconstruct the event data in many ways. This adds significant complexity to the analysis, when compared with traditional "singles" gamma-ray spectroscopy. We are developing an analysis framework to streamline the process so that the analyst can reach a final result within a reasonable time frame.

This software is being developed using the C++ programming language and relies on the library of tools provided by the ROOT framework available on the CERN website (http://root.cern.ch/drupal/), as well as Qt (http://qt.nokia.com/) for graphical user interface functionality. We anticipate drawing upon capabilities developed in two previous PNNL analysis developments, the Coincidence Lookup Library (CLL) for nuclear data (focused on $\gamma$ -$\gamma$ coincidence signatures) (Smith et al., 2004) and the Multi-Isotope Coincidence Analysis code (MICA) (Warren et al., 2006).

The current effort, with the working name "Melusine," consists of a data preprocessor and an analysis engine. The preprocessor (Melusine1) converts measurement results from the native XIA data format into a ROOT data structure. The analysis code (Melusine2) will provide the functionality to analyze both one- and two-dimensional spectra to establish isotope identifications and activity results. This development is in the early phases; current capabilities consist mainly of the preprocessor, various data reconstruction capabilities for both one- and two-dimensional spectra, and peak fitting in one-dimensional spectra. We are currently focused on tasks to simplify both the energy and efficiency calibration for the system.

### Initial Spectroscopic Results

We collected the first spectroscopic data with the array on June 22, 2010. The first results were very encouraging, with all seven channels active. However, initial performance showed significant intermittent high-frequency noise on the baseline for all seven crystals; quiet periods allowed collection of spectra, with several crystals achieving ~3.4-keV FWHM at 1332 keV.

Within several days of collecting these initial results, the loose flange mentioned above was located and tightened, eliminating the intermittent noise. Subsequent tests have shown five crystals operating with energy resolution in the range of 2.2–2.4 keV at 1332 keV, while one crystal cannot be fully biased due to apparent high leakage current, and one crystal continues to suffer from poor energy resolution due to high-frequency noise on the baseline. The crystal with high leakage current can be biased sufficiently to provide ~3.3 keV energy resolution at 1332 keV, and we expect to locate and eliminate the source of noise affecting the other poorly performing crystal. We note that the initial performance of the detector array is better than expected, with useful data available from all seven crystals.

As of this writing, all data has been acquired with the array outside of the shield; the background for these measurements is, understandably, significant. Figure 5 shows a 5-minute background measurement prior to gain matching of the channels. The 1460-keV $^{40}$K peak and the 2615-keV $^{208}$Tl were easily indentified in the spectrum,

and provided a means to gain match the channels, as well as establish a quick energy calibration to verify that the peaks were correctly identified. Figure 6 is a 10-hour room background spectrum, taken after gain matching. The most prominent peak in the spectrum is the 1460-keV peak of $^{40}$K, while the other peaks are associated with the natural uranium and neptunium decay series. Figure 7 shows a close-up of the $^{40}$K peaks for the crystals; five of the crystals show good energy resolution, while broadening of the peak for the two crystals with degraded performance is obvious.

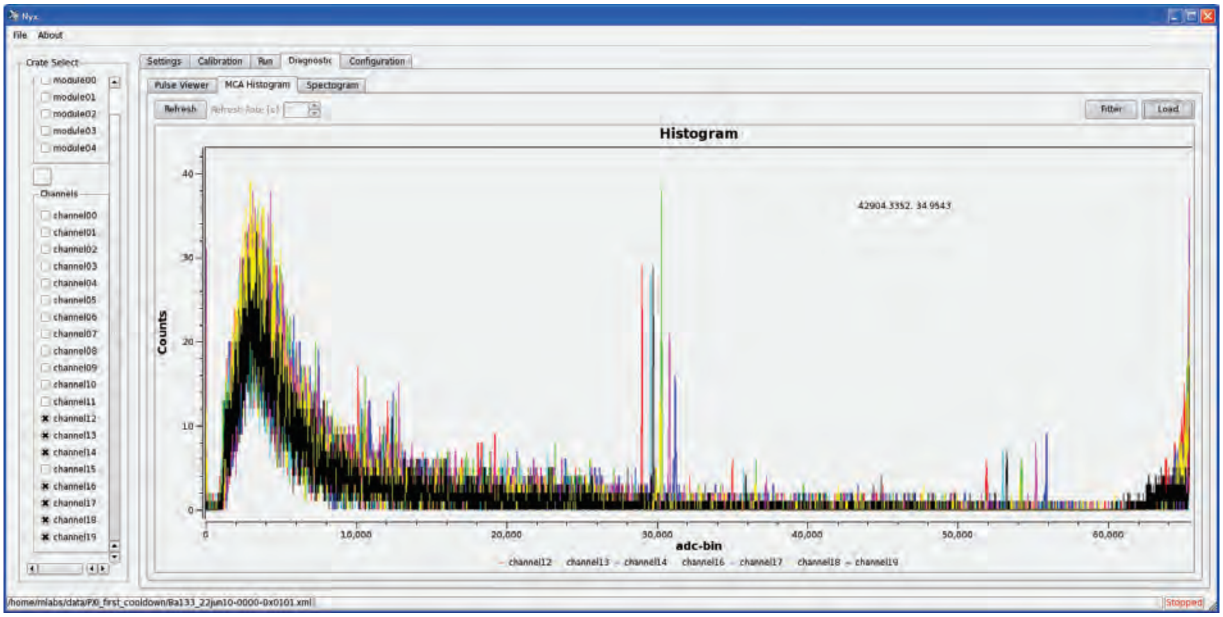


**Figure 5. A 5-minute room background spectrum acquired prior to gain matching the channels. The peaks around channel 30,000 are the 1460 keV $^{40}$K line.**

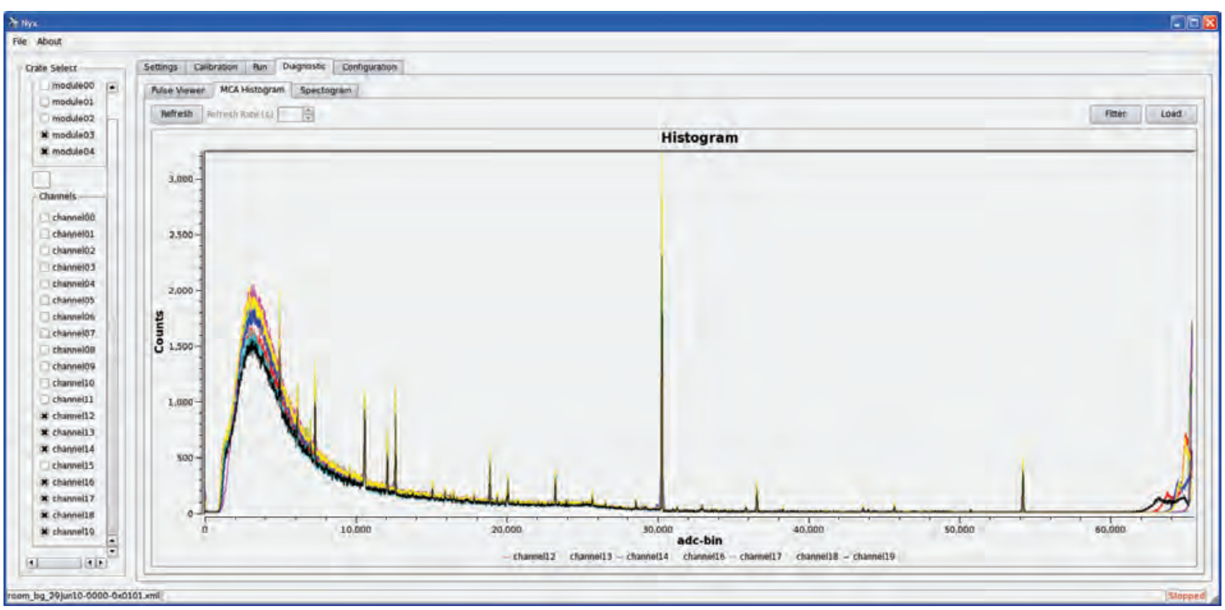


**Figure 6. Room background collected with all seven crystals for 10 hours. The variation in the height of the continuum at low energies appears to be correlated with position of the crystal relative to the nearby shield. The continuum is lowest for those crystals closest to the cave. Data were collected and displayed with NYX.**

Figure 8 and Figure 9 show products from the Melusine analysis package. These are examples of the one-dimensional peak fitting and two-dimensional data reconstructions available with Melusine. The current version of the code still requires setting a number of manual parameters to generate such products; however, we envision a product requiring minimal user intervention to enable rapid analysis of each dataset.

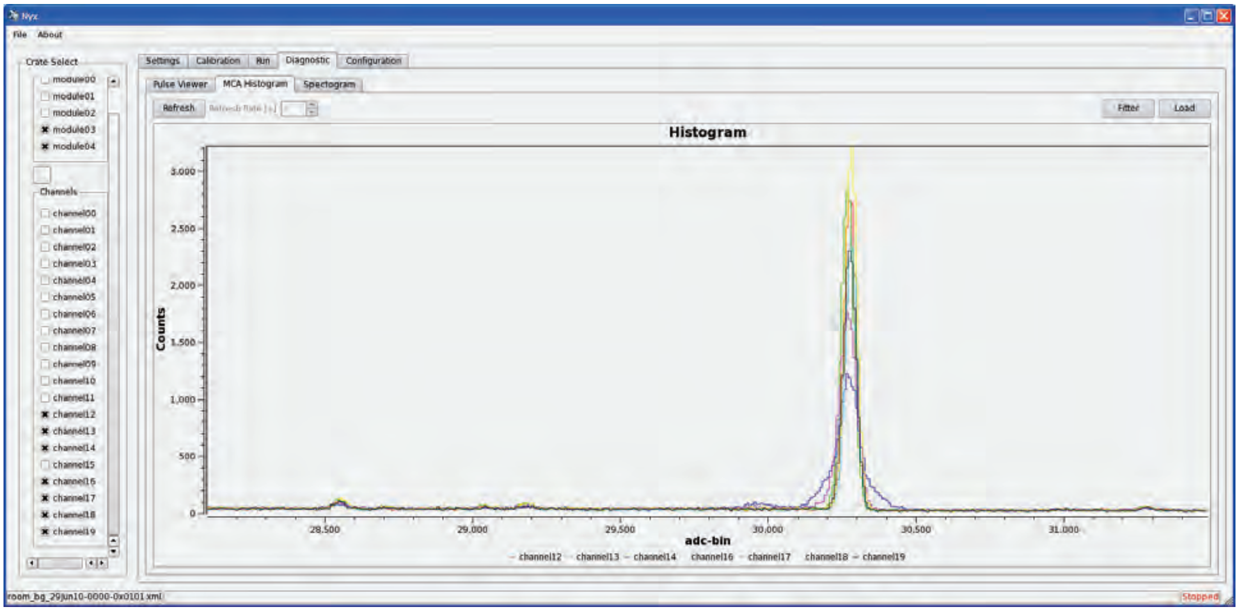


**Figure 7. This figure highlights the $^{40}$K 1460-keV peak from the background spectra of Figure 6. The traces from the two crystals with poorer resolution are apparent.**

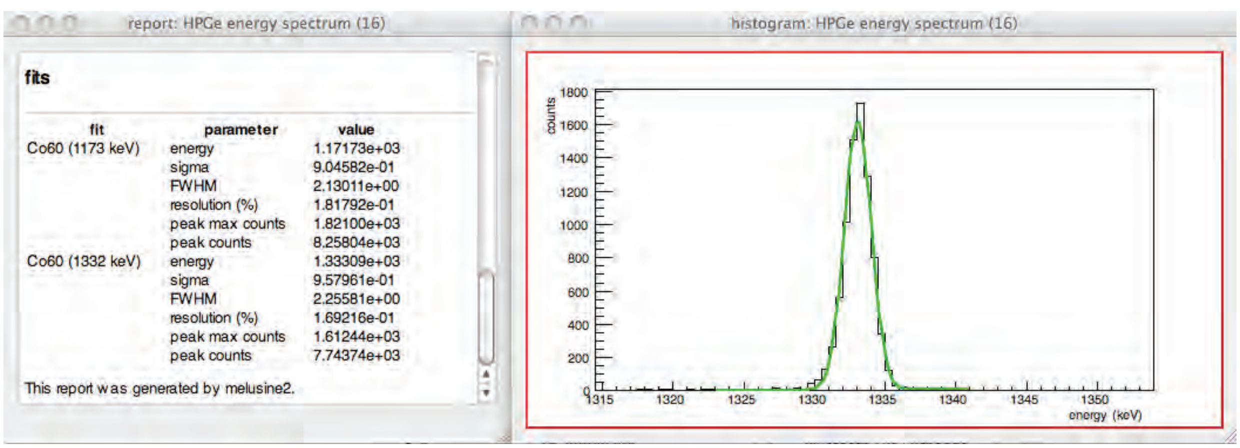


**Figure 8. An analysis product from Melusine2. The image on the right is a fit to a measured $^{60}$Co source peak, while the left-hand panel provides the results for fits to the 1173- and 2332-keV peaks. The energy calibration is off slightly because it is based on a linear fit to one of the other crystals and the rough gain matching discussed earlier in the article.**

**Summed response of outer six crystals**

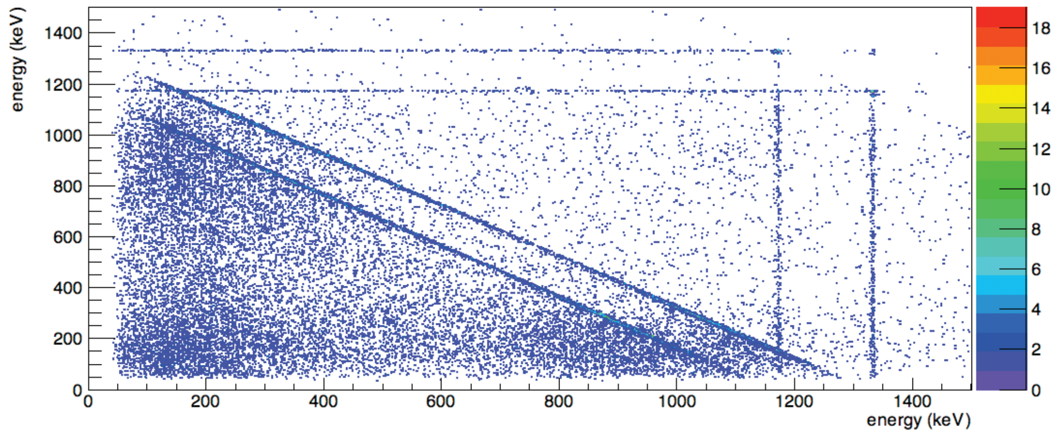


**Figure 9. This figure shows a reconstruction of a short $^{60}$Co measurement; coincidence between detections in the center crystal (x-axis) and event-by-event energy summed detection in the other six crystals (y-axis) is shown. This data reconstruction was produced using Melusine2.**

## CONCLUSIONS AND RECOMMENDATIONS

An array of seven HPGe crystals has been successfully assembled in a cryostat designed and constructed using ultra-low-background materials and techniques. Background performance, as well as the effectiveness of the active anti-cosmic veto, will be determined after the system is moved to a new shallow underground laboratory (~35 m.w.e.) at PNNL. All copper parts for the second cryostat have been electroformed; electron beam welding of subassemblies is in progress.

Initial data collected from this crystal array show that the instrument is functioning extremely well for its debut performance. Five of the crystals perform with energy resolution typical of ultra-low-background cryostats. Elimination of minor remaining ground-loop issues and optimization of the Pixie4 acquisition parameters may allow us to improve upon this performance; however, slightly broadened peaks are expected in ultra-low-background setups due to the long cross arm and potential for increased baseline noise in a multicrystal cryostat. One crystal continues to suffer from significant energy resolution degradation due to high-frequency noise; we hope that the cause of this issue will be straightforward and easily corrected, perhaps something as simple as a bad signal cable. Despite suffering from apparent high-leakage current that is limiting the bias voltage we can apply, the seventh crystal provides useable measurement data.

Collecting this initial data has provided us with valuable measurement datasets to process through the Melusine data analysis package currently under development. This effort is early in its development but can already provide significant capabilities for reconstructing data acquired with the array in multiple ways. Current efforts are focused on streamlining energy and efficiency calibration routines. The long-term vision is that the system will be capable of performing multiple parallel analyses to establish the most sensitive data reconstruction for an isotope-by-isotope measurement.

## REFERENCES

Aalseth, C. E., O. T. Farmer, J. E. Fast, E. W. Hoppe, T. W. Hossbach, J. D. Kephart, K. E. Litke, M. Liezers, H. S. Miley, E. E. Mintzer, and J. S. Reeves (2009). *Nucl. Instrum. Methods Phys. Res. A* (submitted).

Cooper, M. W., C. E. Aalseth, D. A. Haas, J. C. Hayes, J. I. McIntyre, and B. T. Schrom (2010). Digital data acquisition graphical user interface, these Proceedings.

Keillor, M. E., C. E. Aalseth, A. R. Day, J. E. Fast, E. W. Hoppe, T. W. Hossbach, B. J. Hyronimus, H. S. Miley, A. Seifert, and G. A. Warren (2008). Design and construction of an ultra-low-background 14 germanium crystal array for high efficiency and coincidence measurements, in *Proceedings of the 30th Monitoring Research Review: Ground-Based Nuclear Explosion Monitoring Technologies*, LA-UR-08-05261, Vol. 2. pp. 778–786.

Keillor, M. E., C .E. Aalseth, A. R. Day, J. E. Fast, E. W. Hoppe, T. W. Hossbach, B. J. Hyronimus, H. S. Miley, and A. Seifert (2009). Design and construction of an ultra-low-background 14-crystal germanium array for high efficiency and coincidence measurements, *J. Radioanal. Nucl. Chem*. 282: 703–708.

Smith, L. E., E. J. Ellis, A. E. Valsan, C. E. Aalseth, and H. S. Miley (2004). A coincidence signature library for multicoincidence radionuclide analysis systems, *IEEE Trans. Nucl. Sci.* 51: 1044–1048.

Warren, G. A., L. E. Smith, C. E. Aalseth, E. J. Ellis, A. E. Valsan, and W. Mengesha (2006). Generalized multicoincidence analysis methods, *IEEE Trans. Nucl. Sci*. 53: 351–355.